© 2020. Published by The Company of Biologists Ltd | Journal of Experimental Biology (2020) 223, jeb225821. doi:10.1242/jeb.225821

RESEARCH ARTICLE

Nitric oxide produced by periostial hemocytes modulates the bacterial infection-induced reduction of the mosquito heart rate

Tania Y. Estévez-Lao, Leah T. Sigle, Scherly N. Gomez and Julián F. Hillyer*

ABSTRACT

The circulatory and immune systems of mosquitoes are functionally integrated. An infection induces the migration of hemocytes to the dorsal vessel, and specifically, to the regions surrounding the ostia of the heart. These periostial hemocytes phagocytose pathogens in the areas of the hemocoel that experience the highest hemolymph flow. Here, we investigated whether a bacterial infection affects cardiac rhythmicity in the African malaria mosquito, *Anopheles gambiae*. We discovered that infection with *Escherichia coli*, *Staphylococcus aureus* and *Staphylococcus epidermidis*, but not *Micrococcus luteus*, reduces the mosquito heart rate and alters the proportional directionality of heart contractions. Infection does not alter the expression of genes encoding crustacean cardioactive peptide (CCAP), FMRFamide, corazonin, neuropeptide F or short neuropeptide F, indicating that they do not drive the cardiac phenotype. Infection upregulates the transcription of two superoxide dismutase (SOD) genes, catalase and a glutathione peroxidase, but dramatically induces upregulation of nitric oxide synthase (NOS) in both the heart and hemocytes. Within the heart, nitric oxide synthase is produced by periostial hemocytes, and chemically inhibiting the production of nitric oxide using L-NAME reverses the infection-induced cardiac phenotype. Finally, infection induces the upregulation of two lysozyme genes in the heart and other tissues, and treating mosquitoes with lysozyme reduces the heart rate in a manner reminiscent of the infection phenotype. These data demonstrate an exciting new facet of the integration between the immune and circulatory systems of insects, whereby a hemocyte-produced factor with immune activity, namely nitric oxide, modulates heart physiology.

KEY WORDS: *Anopheles gambiae*, Dorsal vessel, Hemolymph, Immunity, Insect, Lysozyme

INTRODUCTION

Nutrients, waste, hormones and other factors are moved throughout the insect hemocoel by hemolymph currents that are maintained by the coordinated action of the muscular pumps of the circulatory system (Hillyer and Pass, 2020). The major driver of hemolymph flow is a dorsal vessel that longitudinally extends along the insect's dorsal midline. In mosquitoes, the posterior portion of the dorsal vessel, the heart, traverses the abdomen and is attached to the dorsal tergum; it generates the forceful contractions that move hemolymph (Andereck et al., 2010; Glenn et al., 2010). The anterior portion of the dorsal vessel, the aorta, joins the heart at the thoraco-abdominal junction and traverses the thorax before terminating in the head (Sigle and Hillyer, 2018b). Although the aorta contracts, it primarily serves as a conduit for hemolymph being propelled by the heart (Sigle and Hillyer, 2018b).

The dorsal vessel of a mosquito periodically alternates between propelling hemolymph in anterograde (towards the head) and retrograde (towards the posterior abdomen) directions (Glenn et al., 2010; League et al., 2015). When the heart contracts anterograde, hemolymph enters the dorsal vessel via six pairs of valves, called ostia, which are located on the anterior portion of abdominal segments 2–7 (Andereck et al., 2010; Barbosa da Silva et al., 2019; Glenn et al., 2010). Wave-like contractions of cardiac muscle move this hemolymph until it exits the vessel via an excurrent opening located in the head (Glenn et al., 2010; Sigle and Hillyer, 2018b). When the heart contracts retrograde, hemolymph enters the dorsal vessel via a pair of ostia located at the thoraco-abdominal junction, and wave-like contractions of heart muscle move this hemolymph until it exits the vessel via an excurrent opening located in the last abdominal segment (Glenn et al., 2010; League et al., 2015).

Although the insect circulatory system is best known for delivering nutrients and maintaining homeostasis, it also plays an essential role in immune defense (Hillyer and Pass, 2020). Hemolymph currents disseminate humoral immune factors and circulate immune cells called hemocytes. In addition to circulating, hemocytes also attach to the integument, the trachea and tracheoles, and internal organs (King and Hillyer, 2013; League and Hillyer, 2016). However, hemocytes are not static; circulating hemocytes can become sessile and enter the circulation (Babcock et al., 2008; Sigle and Hillyer, 2016, 2018a). When an insect is injured, for example, some hemocytes migrate to the wound where they facilitate repair (Babcock et al., 2008; Lai et al., 2001). More strikingly, however, when a mosquito is infected, hemocytes migrate to the heart, where they rapidly and efficiently phagocytose pathogens (King and Hillyer, 2012). Specifically, an infection induces the migration of hemocytes to the areas surrounding the ostia – called the periostial regions – and they preferentially aggregate around the ostia that receive the most flow (King and Hillyer, 2012; Sigle and Hillyer, 2016). By residing in areas of high hemolymph flow, periostial hemocytes are in an ideal position to phagocytose and destroy pathogens that circulate. Although the biology of periostial hemocytes has only been described in detail in mosquitoes, hemocytes have been detected in or on the heart of a stick insect, adult fruit flies, and larvae of the greater wax moth (Cevik et al., 2019; da Silva et al., 2012; Ghosh et al., 2015; Horn et al., 2014; Pereira et al., 2015).

Because intense immune processes occur on the surface of the mosquito heart, we investigated whether an infection alters heart physiology. By means of organismal manipulations and intravital video imaging, we uncovered that a bacterial infection induces the production of nitric oxide by periostial hemocytes, which reduces the heart rate and alters the proportional directionality of heart

Department of Biological Sciences, Vanderbilt University, Nashville, TN 37235, USA.

*Author for correspondence (julian.hillyer@vanderbilt.edu)

J.F.H., 0000-0002-3178-0201

Received 30 March 2020; Accepted 16 June 2020

Journal of Experimental Biology (2020) 223, jeb225821. doi:10.1242/jeb.225821

contractions. Therefore, these data demonstrate a new facet of how the physiologies of the immune and circulatory systems are functionally integrated during the defense against foreign invaders.

MATERIALS AND METHODS

Mosquito rearing

Anopheles gambiae Giles 1902 *sensu stricto* (G3 strain; Diptera: Culicidae) were raised in an insectary under a controlled 12 h:12 h light:dark photoperiod at 27°C and 75% relative humidity (Estevez-Lao et al., 2013). Eggs were hatched in distilled water, and larvae were fed a blend of koi food and baker's yeast. Upon eclosion, adults were maintained on 10% sucrose solution *ad libitum*. All experiments were initiated in female mosquitoes at 3 days post-eclosion.

Bacteria and infections

Mosquitoes were infected with the following bacteria: (1) GFP-expressing, tetracycline-resistant *Escherichia coli* (modified DH5-alpha); (2) *Micrococcus luteus*; (3) *Staphylococcus aureus* (RN 6390); or (4) *Staphylococcus epidermidis* (HIP 04645). Bacteria were grown in Luria–Bertani broth (LB, for *E. coli* and *M. luteus*) or tryptic soy broth (TSB, for *Staphylococcus* spp.), and 0.2 µl of culture dilutions were intrathoracically injected into mosquitoes through the anepisternal cleft using a finely pulled capillary glass needle. The bacterial dose was calculated by plating dilutions of overnight cultures on LB or TSB plates, incubating them overnight at 37°C, and counting the colony forming units (CFUs) 18 h later. Infection doses per mosquito for *E. coli*, *S. aureus* and *S. epidermidis* averaged 91,000, 112,000 and 41,000 CFUs, respectively. *Micrococcus luteus* does not form discrete colonies under our growing conditions, so a precise dose could not be calculated. Instead, *M. luteus* cultures were injected at a normalized optical density at 600 nm (OD_{600}) of 4.2. Using this method of bacterial inoculation, active infections with replicating bacteria ensue for weeks (Brown et al., 2018; Gorman and Paskewitz, 2000; King and Hillyer, 2012). Additional groups that were used in this study were unmanipulated mosquitoes (naïve) and mosquitoes that had been injected with sterile growth medium (injured).

Measurement of heart contraction dynamics

Mosquitoes were anesthetized by cooling in a −20°C environment for 60 s and were then transferred to a Petri dish that was kept on ice. At 1, 3 and 5 days post-treatment, mosquitoes were placed ventral side down with wings spread on Sylgard 184 silicone elastomer plates (Dow Corning, Midland, MI, USA) using the non-invasive method previously described and pictured (Andereck et al., 2010; Glenn et al., 2010). After mosquitoes acclimated to room temperature, 60 s intravital videos of their dorsal abdomens were recorded under bright-field trans-illumination using a Nikon SMZ1500 stereo microscope (Nikon Corporation, Tokyo, Japan) connected to a Hamamatsu ORCA-Flash 2.8 digital CMOS camera (Hamamatsu Photonics, Hamamatsu, Japan) and Nikon Advanced Research NIS-Elements software. Videos were manually analyzed in NIS elements. Specifically, by visualizing the direction and frequency of wake-like contractions of the heart throughout the length of the semi-translucent abdomen, the following physiological parameters were quantified: total, anterograde and retrograde contraction rates (in Hz, which represent contractions per second); the percentage of time the heart spent contracting anterograde and retrograde; the percentage of contractions that propagated anterograde and retrograde; and the frequency of heartbeat directional reversals (Estevez-Lao et al., 2013; Glenn et al., 2010; Hillyer et al., 2014, 2012). For day 1 post-treatment, 45–80 mosquitoes were assayed per treatment. For days 3 and 5 post-treatment, 19–30 and 16–27 mosquitoes were assayed per treatment, respectively. Data were analyzed by two-way ANOVA, followed by a *post hoc* Dunnett's test that compared (i) the injured group at any given time (labeled R for reference) to all other treatment groups for that same time, or (ii) the main effect of a treatment irrespective of day (GraphPad Prism, San Diego, CA, USA). The two-way ANOVA yields three distinct *P*-values: (i) whether treatment had an effect, (ii) whether time had an effect, and (iii) whether the effect of treatment changed with time (interaction).

RNA isolation, cDNA synthesis and real-time quantitative PCR (RT-PCR)

For gene expression analyses in whole bodies, 10–15 mosquitoes were collected at 1 and 5 days after the following treatments: naïve, injury by LB injection, and infection with *E. coli*, *M. luteus*, *S. aureus* or *S. epidermidis*. Mosquitoes were homogenized in TRIzol reagent (Invitrogen, Carlsbad, CA, USA), RNA was then re-purified using the PureLink Micro-to-Midi total RNA purification system (Invitrogen), and up to 5 µg of RNA was treated with RQ1 RNase-free DNAse (Promega, Madison, WI, USA). First-strand cDNA was synthesized using an oligo dT primer and the SuperScript III First-Strand Synthesis System (Invitrogen). Relative quantification (RQ) of mRNA levels was performed using gene-specific primers and Power SYBR Green PCR Master Mix (Applied Biosystems, Foster City, CA, USA) on a CFX Connect Real-Time Detection System (Bio-Rad, Hercules, CA, USA). The thermal cycle conditions used were: 50°C for 2 min, initial denaturation at 95°C for 10 min, followed by 40 cycles of 95°C for 15 s and 60°C for 1 min. Melting curve analysis after RT-PCR confirmed the specificity of the primers and that the cDNAs were devoid of genomic DNA contamination. The relative amount of mRNA was calculated using the $2^{-\Delta\Delta C_t}$ method, and the results were normalized with *A. gambiae* ribosomal protein S7 (*RPS7*) as an internal housekeeping gene (Coggins et al., 2012; Estevez-Lao et al., 2013; Livak and Schmittgen, 2001). Ribosomal protein 17 (*RPS17*) was used as a control gene in order to validate the *RPS7* reference, as we have done in the past (Coggins et al., 2012; Estevez-Lao et al., 2013). The average fold-change in mRNA level was calculated relative to naïve mosquitoes at 1-day post-treatment. Between three and five biological replicates were conducted and each was analyzed in duplicate. The one exception was lysozyme C2 (*LYSC2*), for which two biological replicates were done.

For gene expression analysis in dissected tissues, cDNA was synthesized from 12 hearts, 12 abdominal carcasses, and hemocytes (hemolymph) from 25 mosquitoes. Samples were collected at 1 day post-treatment, and the treatments were naïve, injury by LB injection, or infection with *E. coli*. Hearts were isolated by making an incision in the abdomen along the pleural membrane, removing the internal organs, and resecting the heart using 0.2 mm diameter minuten pins. Attached to these hearts are periostial hemocytes, pericardial cells and some alary muscles (Sigle and Hillyer, 2018a). The remainder of the abdomen is called the carcass and contains abdominal muscle, fat body, sessile hemocytes not associated with the heart, the ventral nerve cord, the integument and other cells that attach to the integument (Andereck et al., 2010; King and Hillyer, 2013). Therefore, the abdominal carcasses are devoid of the heart, pericardial cells, periostial hemocytes and internal organs such as the midgut and ovaries. Heart and abdominal carcass samples were placed in TRIzol and processed as above. Hemocytes

were collected by volume displacement, also known as perfusion (Hillyer and Christensen, 2002; Hillyer and Estévez-Lao, 2010). Specifically, a small tear was made in the penultimate abdominal segment, phosphate-buffered saline (PBS, pH 7.2) was injected using a microcapillary glass needle inserted through the dorsal cervical membrane, and the hemolymph that exited through the posterior abdomen was directly collected into a microfuge tube containing lysis buffer with 2% β-mercaptoethanol. The RNA was then purified using the PureLink Micro-to-Midi total RNA purification system and processed as described above. The average fold-change in mRNA level was calculated relative to the naïve group of each individual tissue. Three biological trials were conducted – except for hemocytes, where two biological trials were performed – and each was analyzed in duplicate.

The genes assayed were five cardioregulatory genes, five genes related to reactive oxygen or nitrogen species, two lysozymes, one control gene and the reference gene. These genes were crustacean cardioactive peptide (*CCAP*; JX880074, AGAP009729), FMRFamide (*FMRFamide*; KJ583231, KJ583232, AGAP005518), corazonin (*CRZ*; AGAP003675), neuropeptide F (*NPF*; AGAP004642), short neuropeptide F (*sNPF*; DQ437578), nitric oxide synthase (*NOS*; AGAP029502), copper-zinc superoxide dismutase 2 (*CuSOD2*; AGAP005234), copper-zinc superoxide dismutase 3 (*CuSOD3*; AGAP010347), catalase 1 (*CAT1*; AGAP004904), glutathione peroxidase 3 (*GPXH3*; AGAP004248), lysozyme C1 (*LYSC1*; AGAP007347), *LYSC2* (AGAP007343), *RPS17* (AGAP004887) and *RPS7* (AGAP010592). Gene IDs that start with AGAP are from VectorBase (www.vectorbase.org) whereas others are from GenBank (www.ncbi.nlm.nih.gov/genbank). The primers used in this study are listed in Table S1. Genes were considered regulated when the fold-change was ≤0.5 or ≥2.

Inhibition of nitric oxide synthase activity and quantification of nitrite

Either the chemical inhibitor of nitric oxide production, *N*ω-nitro-L-arginine methyl ester hydrochloride (L-NAME; Sigma-Aldrich, St Louis, MO, USA), or its inert enantiomer *N*ω-nitro-D-arginine methyl ester hydrochloride (D-NAME; Sigma-Aldrich), was mixed with *E. coli* or *S. aureus* for a final concentration of 100 mmol l^{-1}, and then intrathoracically injected into mosquitoes (Hillyer and Estévez-Lao, 2010). Additional mosquitoes were injured or infected with bacteria in the absence of these chemicals. At 1 day post-treatment, videos of contracting hearts were acquired and the total contraction rate was calculated. In parallel, the hemolymph from 20–25 mosquitoes was extracted by centrifugation using a protocol described for mosquito larvae and adults (League et al., 2017). Briefly, a small tear was made in the penultimate abdominal segment, and a group of mosquitoes was placed inside a 0.6 ml microfuge tube that had a small incision in the bottom. This tube was inserted into a 1.5 ml microfuge tube and centrifuged at 1500 ***g*** for 5 min at 4°C. The 2–3 µl of hemolymph collected was used to quantify the amount of nitric oxide produced by measuring the accumulation of nitrite (NO_2^-; a breakdown product of nitric oxide) using a modified Griess reaction method (Giustarini et al., 2008) and the instructions provided with the Griess kit (Invitrogen). In this colorimetric assay, 1 µl of hemolymph was added to 49 µl of 62.5% of ethanol and mixed with 30 µl of Griess solution (1% sulfanilamide, 0.1% naphtyl-ethylendiamine and 5% phosphoric acid). Following a 30 min incubation at room temperature in darkness, the absorbance of each sample was measured at 550 nm using a Biophotometer Plus spectrophotometer (Eppendorf, Hamburg, Germany). A standard curve was generated with sodium nitrite in concentrations ranging from 1 to 100 µmol l^{-1}, and sample values were expressed as micromoles of nitrite per mosquito. For heart rate experiments, three independent trials were conducted. For nitrite measurements, four to six independent trials were conducted, each with two samples. Data were analyzed by ANOVA, followed by Dunnett's multiple comparisons test.

NADPH diaphorase histochemical bioassay

Nitric oxide synthase (NOS) activity was determined by NADPH diaphorase staining, whereby the diaphorase enzymatic activity of NOS reduces tetrazolium dyes to a dark blue formazan precipitate in the presence of NADPH (Gonzalez-Zulueta et al., 1999). The procedure was similar to how we have stained NOS activity in circulating hemocytes following perfusion (Hillyer and Estévez-Lao, 2010), except that here it was conducted on dissected abdomens that included the heart and associated tissues. Briefly, mosquitoes were injected with 16% paraformaldehyde (Electron Microscopy Sciences, Hatfield, PA, USA), and 5 min later were immersed in PBS containing 0.1% Tween 20 and the abdomen dissected along a coronal plane. Dorsal abdomens containing the heart were transferred to 2 ml microfuge tubes and washed in 50 mmol l^{-1} Tris-buffered saline (TBS, pH 7.2) for 10 min in an orbital shaker, fixed again in 4% paraformaldehyde for 30 min, and washed three times for 10 min each in TBS. After 15 min of permeabilization in 0.2% Triton X-100 in TBS, the abdomens were washed and then incubated for 90 min at 37°C in a mixture containing 1 mmol l^{-1} β-NADPH, 0.2 mmol l^{-1} nitroblue tetrazolium, 0.2% Triton X-100 and 0.02% sodium azide in TBS. The staining process was stopped by washing tissues several times in TBS, and each dorsal abdomen was mounted on a microscope slide using Aqua-Poly/Mount (Polysciences Inc., Warrington, PA, USA). Slides were viewed under bright-field illumination using a Nikon 90i compound microscope connected to a Nikon DS-Fi1 high-resolution color CCD camera and NIS-Elements software. Approximately 10 abdomens were processed per treatment, distributed in three independent biological replicates.

Treatment with lysozyme

Chicken lysozyme (MP Biomedicals, Solon, OH, USA) was reconstituted at 1×10^{-5} mol l^{-1} and 1×10^{-3} mol l^{-1} in PBS and 0.2 µl injected into mosquitoes. An additional group was injured by injecting PBS. Videos of contracting hearts were acquired at 3 h (between 23 and 26 mosquitoes per group) and 24 h (between 26 and 27 mosquitoes per group) after treatment, and the total contraction rate was calculated. Three independent trials were conducted, and data were analyzed by two-way ANOVA followed by Dunnett's multiple comparisons test.

RESULTS

A bacterial infection reduces heart contraction rate

At 1 day following injection (when mosquitoes were 4 days old) the total heart rate in injured mosquitoes averaged 2.02 Hz, and at 3 and 5 days following injection it averaged 2.19 and 2.24 Hz, respectively (Fig. 1A). Infection for 1 day with *E. coli*, *S. aureus* and *S. epidermidis* reduced the heart rate relative to injured mosquitoes by 13, 18 and 7%, respectively, and infection for 3 days with these three bacterial species reduced the heart rate by 16, 24 and 25%, respectively (Fig. 1A). By 5 days, *S. aureus* was the only infection that significantly reduced the heart rate, and did so by 17%. Infection with *M. luteus* had a negligible effect, or no effect, on heart rate. Finally, relative to naïve mosquitoes, injury resulted in a modest 5.6% increase in mosquito heart rate (main injury effect:

Journal of Experimental Biology (2020) 223, jeb225821. doi:10.1242/jeb.225821

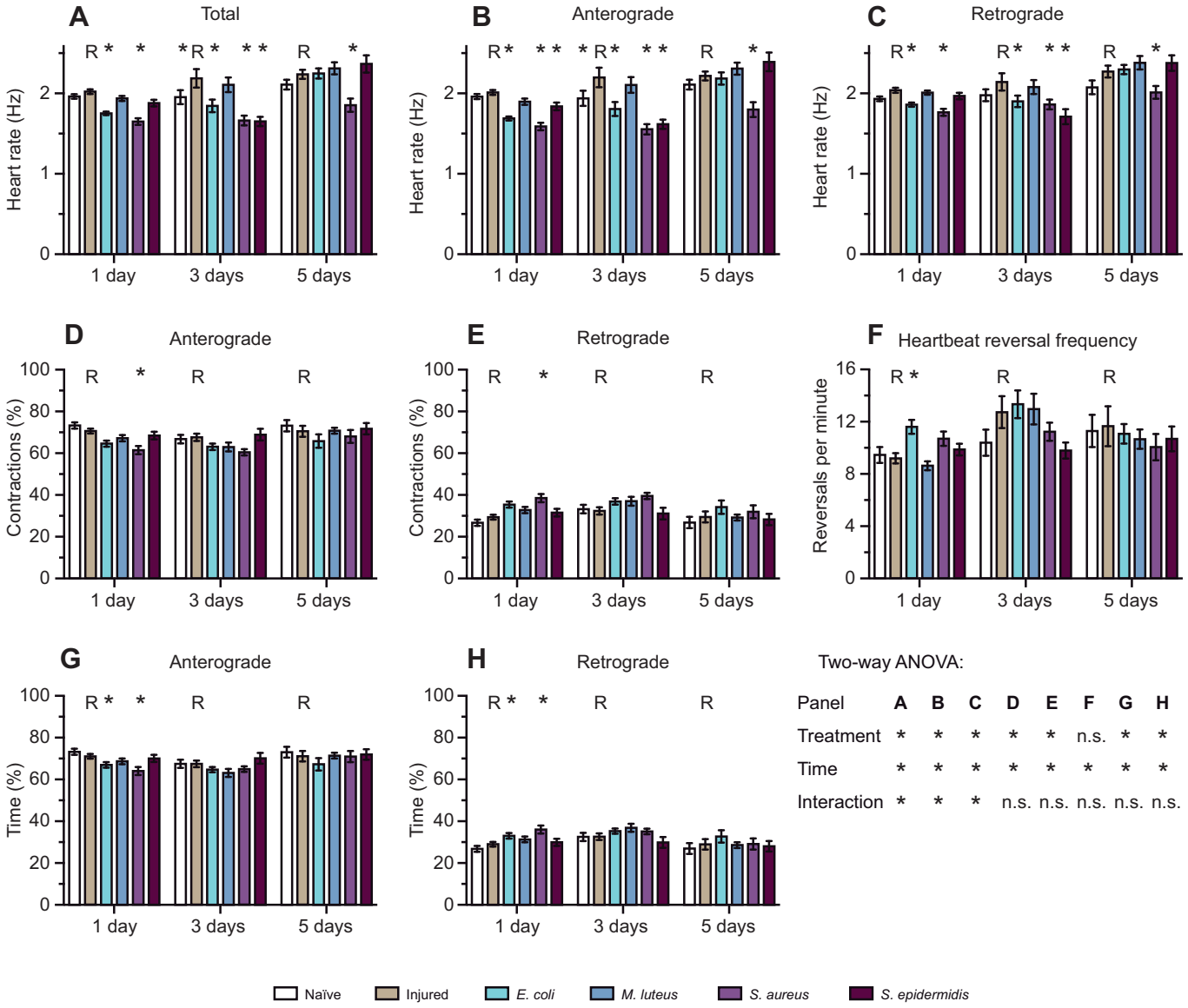

Fig. 1. Effect of infection on heart physiology. (A–C) Total (A), anterograde (B) and retrograde (C) contraction rates at 1, 3 and 5 days after treatment in naïve mosquitoes, injured mosquitoes and mosquitoes infected with *E. coli*, *M. luteus*, *S. aureus* or *S. epidermidis*. (D,E) Percentage of contractions propagating in the anterograde (D) and retrograde (E) directions. (F) Frequency of heartbeat directional reversals. (G,H) Percentage of time spent contracting in the anterograde and retrograde directions. The graphs display means±s.e.m. Data were analyzed by two-way ANOVA followed by Dunnett's *post hoc* test. 'R' above a column denotes the reference; **P*<0.05 when compared with the reference; n.s., not significant. Sample sizes are presented in Table S2.

P=0.01), which is consistent with our earlier observations (Estevez-Lao et al., 2013; Hillyer et al., 2014, 2012).

When heart rate was analyzed independently for anterograde and retrograde contractions, a similar pattern was observed (Fig. 1B,C). Infection with *E. coli* (main anterograde and retrograde effects: *P*<0.0001 and *P*=0.0168, respectively), *S. aureus* (*P*<0.0001 and *P*<0.0001) and *S. epidermidis* (*P*=0.003 and *P*=0.047), but not *M. luteus* (*P*=0.928 and *P*=0.999), decreased the anterograde and retrograde heart rate. Moreover, injury resulted in a small increase in both the anterograde and retrograde heart rate (*P*=0.024 and *P*=0.004). Therefore, we conclude that an infection reduces the total, anterograde and retrograde heart rates.

The percentage of contractions that propagated in the anterograde direction in injured mosquitoes was 71, 68 and 71% at 1, 3 and 5 days after injection, respectively (Fig. 1D). Likewise, the percentage of time the heart of injured mosquitoes spent contracting in the anterograde direction was 71, 67 and 71% at 1, 3 and 5 days after injection, respectively (Fig. 1G). The similarities between the percentage of contractions and the percentage of time in any given direction are because the anterograde and retrograde heart rates are similar. Relative to injured mosquitoes, infected mosquitoes contracted less and spent less time contracting in the anterograde direction (Fig. 1D,G). This was most noticeable in mosquitoes infected with *E. coli* or *S. aureus*, where at 1 day after treatment the percentage of time spent contracting in the anterograde direction was 4 and 7 percentage points lower, respectively, than in injured mosquitoes. As a consequence, infected mosquitoes contracted more, and spent more time contracting, in the retrograde direction (Fig. 1E,H). Finally, relative to naïve mosquitoes, injury did not alter the percentage of contractions or time spent contracting in any given direction.

Journal of Experimental Biology (2020) 223, jeb225821. doi:10.1242/jeb.225821

The heart of injured mosquitoes reversed contraction direction 9.2, 12.7 and 11.7 times per minute at 1, 3 and 5 days after injection, respectively (Fig. 1F). Infection did not have a consistent or predictable effect on the frequency of heartbeat reversals (Fig. 1F), which was not surprising because this is the most fluctuating cardiac parameter we measure (Doran et al., 2017; Estevez-Lao et al., 2013; Glenn et al., 2010; Hillyer et al., 2014, 2012). Therefore, we conclude that infection has a negligible effect on the frequency of heartbeat reversals.

The transcription of genes encoding cardiomyotropic peptides is not meaningfully affected by infection

To begin to uncover the molecular drivers of the infection-induced reduction in heart rate, we assayed the expression of cardiomyotropic factors in the whole bodies of naïve mosquitoes, injured mosquitoes and mosquitoes infected with *E. coli*, *M. luteus*, *S. aureus* or *S. epidermidis* for 1 or 5 days. In addition, we repeated this experiment but instead measured gene expression in the heart, the circulating hemocytes, the abdominal carcass and the whole body of mosquitoes that were naïve, injured or infected with *E. coli* for 1 day. Attached to the heart were the periostial hemocytes, pericardial cells and alary muscles (Sigle and Hillyer, 2018a), and attached to the abdominal carcass were the non-periostial sessile hemocytes (King and Hillyer, 2013). Many factors that affect heart rhythmicity have been identified in insects (Chowański et al., 2016; Hillyer, 2018), and here we focused on five genes encoding neuropeptides. *CCAP* and *FMRFamide* affect circulatory physiology in mosquitoes (Estevez-Lao et al., 2013; Hillyer et al., 2014), *NPF* and *sNPF* modulate heart physiology in *Drosophila* (Setzu et al., 2012), and *CRZ* modulates heart physiology in some insects but not others (Boerjan et al., 2010; Hillyer et al., 2012).

RT-PCR experiments showed that at 1 day post-treatment, there was no meaningful change in the mRNA abundance of *CCAP*, *FMRFamide*, *CRZ*, *NPF* or *sNPF* (no ≤0.5-fold or ≥2-fold change; Figs 2 and 3). At 5 days post-infection, there was a general elevation in the mRNA abundance of some of these factors relative to naïve mosquitoes of the same age (Fig. 2), but changes were insufficient to explain the cardiac phenotype because (i) the phenotype would be explained by a decrease in mRNA abundance instead of an increase, (ii) the tissue-specific experiments did not show a meaningful change in transcription following infection (Fig. 3), and (iii) mRNA abundance of *FMRFamide* and *sNPF* were undetectable in the heart and circulating hemocytes (Fig. 3B,E). The one possible exception is *CRZ* because infection increased the mRNA level in the carcass (Fig. 3C), but the corazonin peptide has a negligible effect on mosquito heart physiology (Hillyer et al., 2012).

NOS and other genes encoding enzymes involved in oxidative stress are transcriptionally upregulated in the heart following infection

Because the mRNA abundance of cardiomyotropic peptides did not explain the cardiac phenotype, we turned our attention to nitric oxide synthase. NOS produces nitric oxide, which is a pleiotropic molecule that, in both vertebrates and invertebrates, has anti-microbial activity (Gupta et al., 2009; Hillyer and Estévez-Lao, 2010; Hughes, 2008; Luckhart et al., 1998; Rivero, 2006). This free radical is also a vasodilator and heartbeat modulator in vertebrate animals (Rastaldo et al., 2007; Smiljic et al., 2014), and at least in a stick insect, nitric oxide reduces the heart rate (da Silva et al., 2012).

RT-PCR experiments using cDNAs from whole body showed that *NOS* is transcriptionally upregulated at both 1 and 5 days following all infections tested (Fig. 4A). This increase was more pronounced at 1 day post-infection, where *NOS* mRNA level was

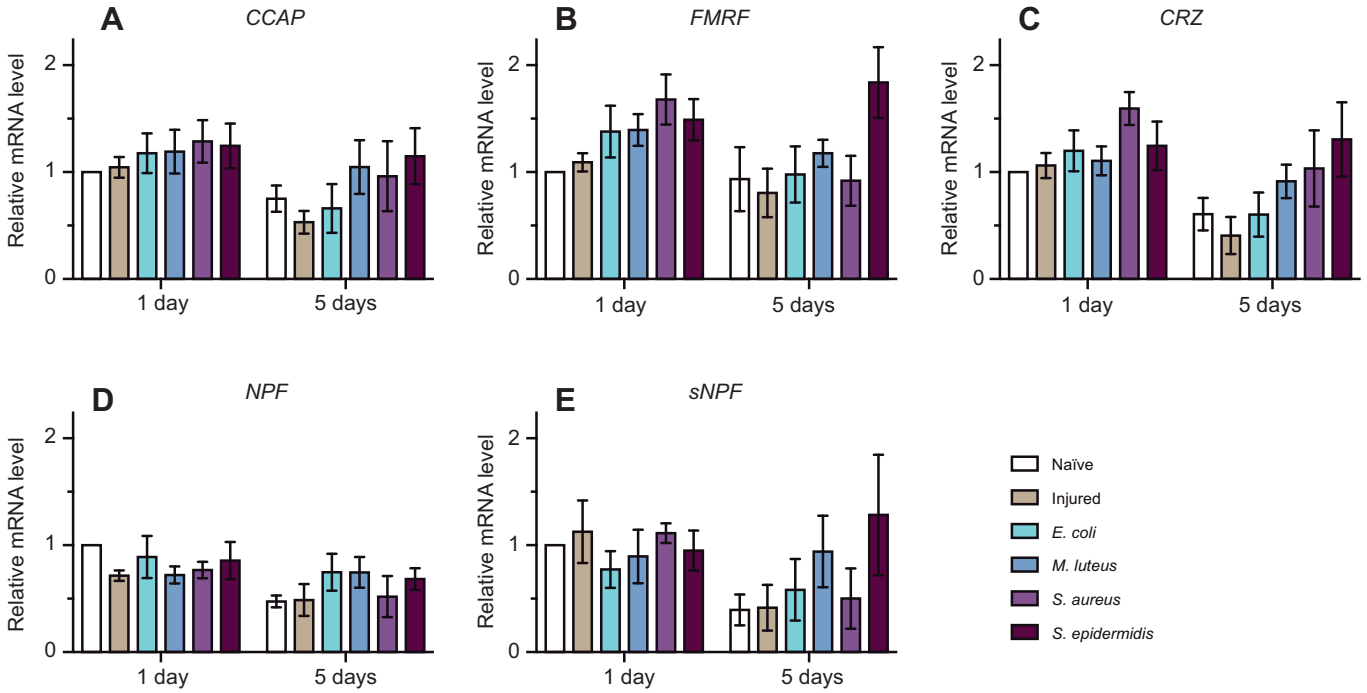

Fig. 2. Effect of infection on the expression of genes encoding myotropic peptides in the whole body. Relative gene expression of *CCAP* (A), *FMRFamide* (B), *CRZ* (C), *NPF* (D) and *sNPF* (E) measured by RT-PCR at 1 and 5 days after treatment in naïve mosquitoes, injured mosquitoes and mosquitoes infected with *E. coli*, *M. luteus*, *S. aureus* or *S. epidermidis*. The graphs display mean±s.e.m. fold-change in mRNA levels relative to naïve mosquitoes at 1 day post-treatment, using *RPS7* as the reference gene. Sample sizes are presented in Table S2.

Journal of Experimental Biology (2020) 223, jeb225821. doi:10.1242/jeb.225821

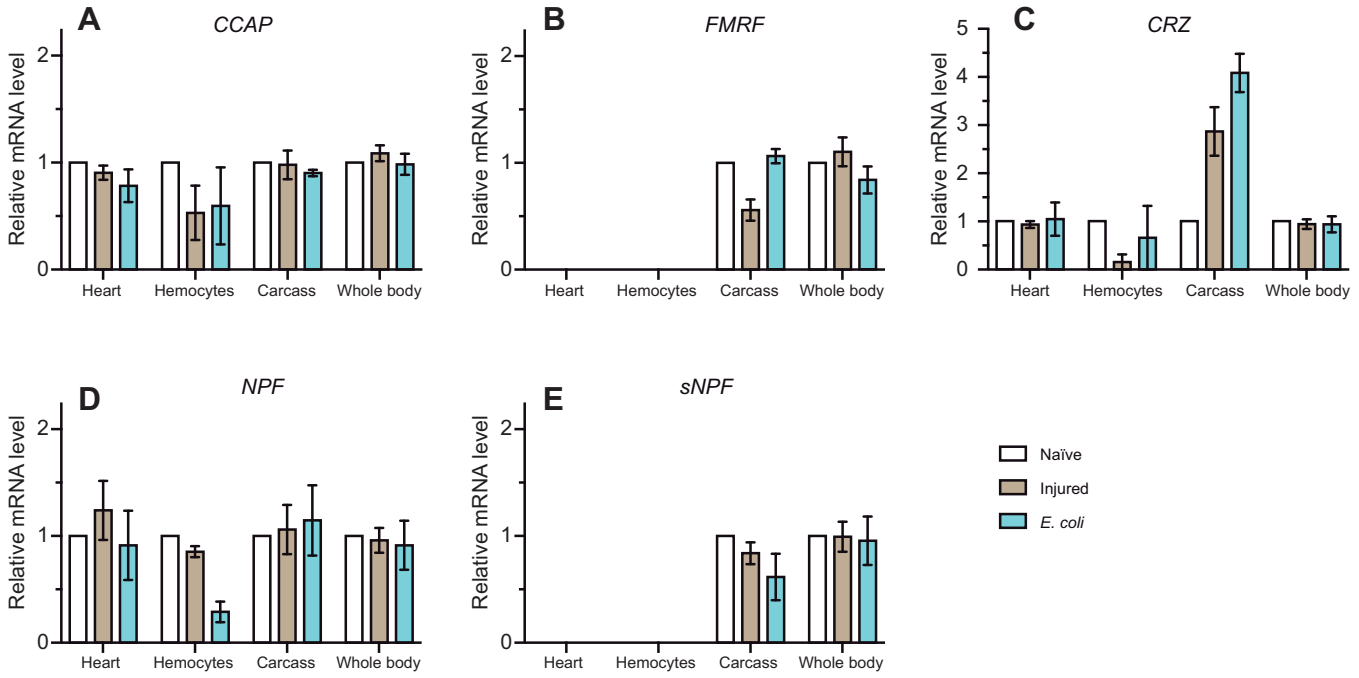

Fig. 3. Effect of infection on the expression of genes encoding myotropic peptides in the heart, hemocytes, carcass and whole body. Relative gene expression of *CCAP* (A), *FMRFamide* (B), *CRZ* (C), *NPF* (D) and *sNPF* (E) measured by RT-PCR at 1 day after treatment in naïve, injured and *E. coli*-infected mosquitoes. The graphs display mean±s.e.m. fold-change in mRNA levels relative to the naïve group of each tissue, using *RPS7* as the reference gene. Sample sizes are presented in Table S2.

>8-fold higher in mosquitoes infected with *E. coli* and *S. aureus* relative to naïve mosquitoes. When tissues were independently analyzed, *NOS* mRNA in infected mosquitoes was also enriched in the heart (7.7-fold), circulating hemocytes (9.9-fold) and carcass (19-fold), relative to naïve mosquitoes (Fig. 5A).

Other free radicals have been implicated in modulating heart physiology. In vertebrates, reactive oxygen species (ROS) drive age-associated changes in the vascular wall (El Assar et al., 2013). In insects, they also have immune function, including in the mosquito response to malaria parasites (Bahia et al., 2013; Herrera-Ortiz et al., 2011; Molina-Cruz et al., 2008; Surachetpong et al., 2011). Therefore, we also used RT-PCR to measure mRNA abundance of *CuSOD2*, *CuSOD3*, *CAT1* and *GPXH3*. Although following a bacterial infection none was highly regulated in the mosquito whole body (Fig. 4B–E), mild increases in mRNA abundance were detected in tissues (Fig. 5B–E). For example, a modest increase in the mRNA abundance of *CuSOD3* (2.1-fold) was observed in the heart following infection. Moreover, in the carcass, *CuSOD2* (2.0-fold) and *CAT1* (2.2-fold) were enriched after infection, and in the hemocytes, *CuSOD2* (3.1-fold) and *CuSOD3* (2.8-fold) mRNA abundance also increased with infection. To ensure that changes were not global, we measured the expression of the housekeeping gene, *RPS17*. Neither treatment nor tissue had an impact on mRNA abundance of *RPS17*.

Blocking nitric oxide production reverses the infection-induced reduction of the heart rate

To test whether NOS alters heart physiology, we infected mosquitoes with *E. coli* or *S. aureus* in the presence or absence of the inhibitor of nitric oxide production, L-NAME, or its inert enantiomer, D-NAME (Luckhart et al., 1998; Rees et al., 1990). We then tested whether reducing nitric oxide production reverses the infection-induced cardiac phenotype (Fig. 6A). In the trials involving *E. coli*, infection decreased the heart rate by 8%, and this was completely reversed when *E. coli* was co-injected with L-NAME but not when it was co-injected with D-NAME. In the trials involving *S. aureus*, infection decreased the heart rate by 17%, and this was mostly reversed when *S. aureus* was co-injected with L-NAME but not when it was co-injected with D-NAME.

We then sought to confirm that the blocking of nitric oxide production was unique to treatment with L-NAME (Fig. 6B). Nitric oxide is an unstable free radical, so instead of quantifying nitric oxide in the hemolymph, we measured the accumulation of one of its breakdown products, nitrite (Hughes, 2008; Kelm, 1999; Rivero, 2006). Relative to injured mosquitoes, an infection with *E. coli* or *S. aureus* increased nitrite in the hemolymph by 70 and 36%, respectively. However, when these infected mosquitoes were also treated with L-NAME, nitrite dropped by 63 and 47%, respectively, with these levels being even lower than those observed in injured mosquitoes. Finally, treatment of infected mosquitoes with D-NAME resulted in a non-significant reduction in nitrite levels. Therefore, infection induces the production of nitric oxide, and as predicted, this is reversed by L-NAME but not D-NAME. Together with the intravital video imaging experiments, we conclude that chemically inhibiting nitric oxide production reverses the infection-induced reduction of heart rate.

Nitric oxide synthase and nitric oxide are produced by periostial hemocytes

Having determined that nitric oxide reduces heart rate, we investigated which cells produce this free radical. We did so by means of NADPH diaphorase staining, whereby NOS catalyses a reaction that results in a dark blue or purple precipitate (Gonzalez-Zulueta et al., 1999; Hillyer and Estévez-Lao, 2010). Examination of dorsal abdomens of naïve or injured mosquitoes using bright-field illumination revealed negligible NADPH diaphorase staining,

Journal of Experimental Biology (2020) 223, jeb225821. doi:10.1242/jeb.225821

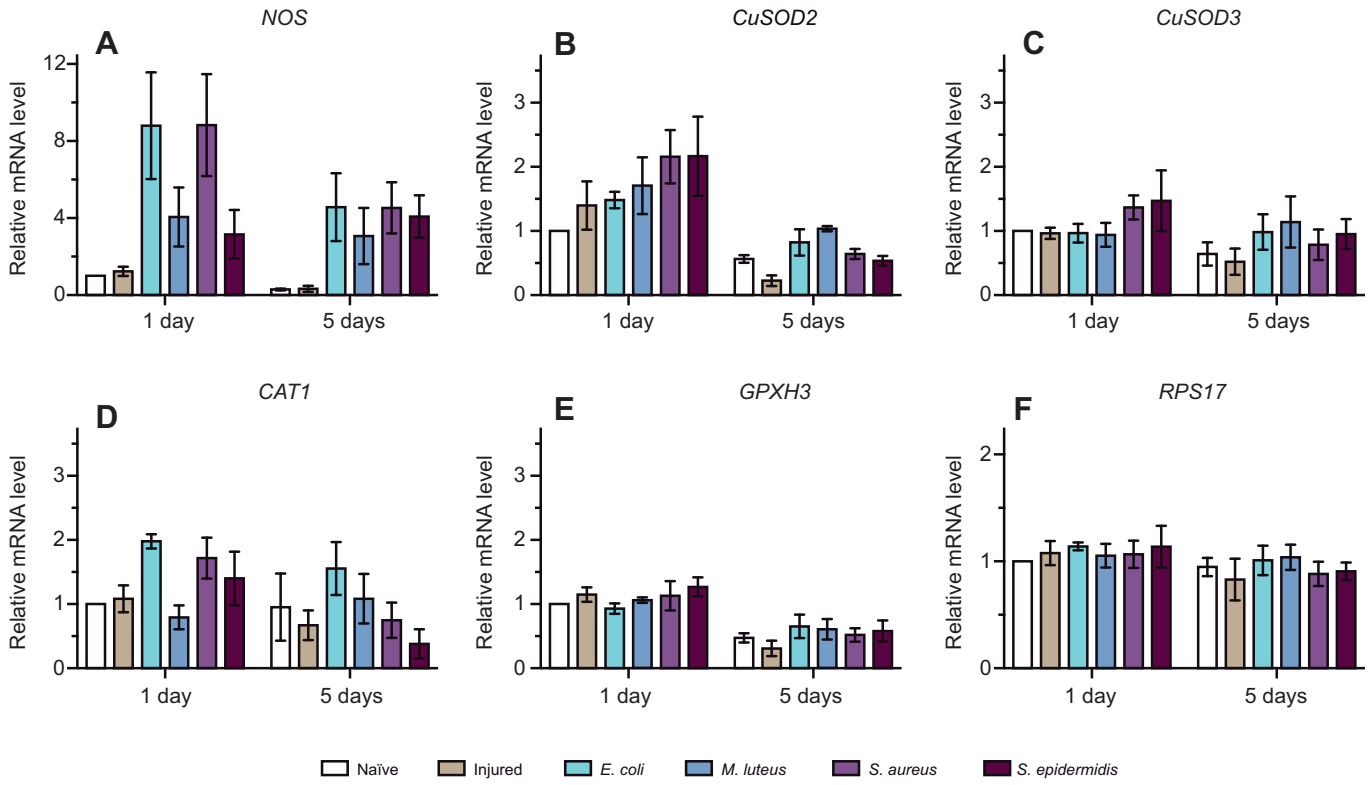

Fig. 4. Effect of infection on the expression of genes encoding enzymes involved in oxidative stress in the whole body. Relative gene expression of *NOS* (A), *CuSOD2* (B), *CuSOD3* (C), *CAT1* (D), *GPXH3* (E) and *RPS17* (F; control), measured by RT-PCR at 1 and 5 days after treatment in naïve mosquitoes, injured mosquitoes and mosquitoes infected with *E. coli*, *M. luteus*, *S. aureus* or *S. epidermidis*. The graphs display mean±s.e.m. fold-change in mRNA levels relative to naïve mosquitoes at 1 day post-treatment, using *RPS7* as the reference gene. Sample sizes are presented in Table S2.

indicating that in these tissues there is undetectable NOS activity, and by extension, negligible nitric oxide production (Fig. 7A,B). When infected mosquitoes were examined, their dorsal abdomens had intense NADPH diaphorase staining (Fig. 7C–F). This staining strongly concentrated in flanking foci located in the anterior of each abdominal segment along the longitudinal midline of the tergum. This location matches the location of the ostia and the periostial hemocytes (King and Hillyer, 2012; Sigle and Hillyer, 2016). Bright-field imaging at higher magnification to view cell size and shape, together with fluorescence illumination to view GFP-expressing *E. coli*, confirmed that the cells with NOS activity – and therefore the nitric oxide producers – are the periostial hemocytes (Fig. 7G).

Lysozyme reduces the heart rate

Having uncovered a role for nitric oxide in mosquito heart physiology, we assayed whether lysozymes are also involved in the observed cardiac phenotype. We targeted lysozymes because in canines, lysozyme induces the production of hydrogen peroxide (H_2O_2), which activates endothelial NOS (eNOS) and triggers myocardial depression (Mink et al., 2009). RT-PCR experiments in mosquito whole bodies showed that mRNA abundance of *LysC1* and *LysC2* is upregulated at 1 day (up to 12- and 44-fold, respectively) and 5 days (up to 7- and 39-fold, respectively) following infection with all bacterial species (Fig. 8A). Moreover, both *LysC1* (205-fold) and *LysC2* (11-fold) are highly upregulated in the heart following infection with *E. coli* (Fig. 8B).

With lysozymes as promising targets, we tested whether treating mosquitoes with commercially purchased chicken lysozyme in the absence of infection mimics the infection-induced cardiac phenotype. At 3 h after treatment with chicken lysozyme at 1×10^{-5} and 1×10^{-3} mol l^{-1}, the heart rate was reduced by 10 and 15%, respectively, relative to injured mosquitoes (Fig. 8C). At 24 h after treatment, however, lysozyme had no effect on heart rate, presumably because the injected lysozyme had been depleted (Fig. 8C). Therefore, because treatment with lysozyme results in a phenotype that resembles the infection-induced reduction in heart rate, we infer that lysozymes modulate cardiac function.

DISCUSSION

The insect heart is myogenic, but its rhythmicity is modulated by endogenous and exogenous factors (Hillyer and Pass, 2020). Endogenous or biotic factors that affect heart physiology include neuropeptides and neurotransmitters (Chowański et al., 2016; Hillyer, 2018). Exogenous or abiotic factors that affect heart physiology include age, nutritional and hydration status, and the thermal environment (Doran et al., 2017; Ellison et al., 2015; Richards, 1963). One aspect that has gone largely unexplored is whether an infection alters heart physiology. This merits investigation because the circulatory and immune system of insects – and Pancrustacea in general – are functionally integrated (Hillyer, 2015). This functional integration is most clearly documented in mosquitoes, where an infection induces the migration of hemocytes – and their phagocytic response – to the heart and nowhere else in the body (King and Hillyer, 2012, 2013; Sigle and Hillyer, 2016, 2018a). In at least flies, moths and stick insects, hemocytes or pathogens also aggregate in or on the heart (Cevik et al., 2019; da Silva et al., 2012; Ghosh et al., 2015; Horn et al., 2014; Pereira et al., 2015). In the present study, we uncovered that an infection decreases the heart rate of mosquitoes and increases

Journal of Experimental Biology (2020) 223, jeb225821. doi:10.1242/jeb.225821

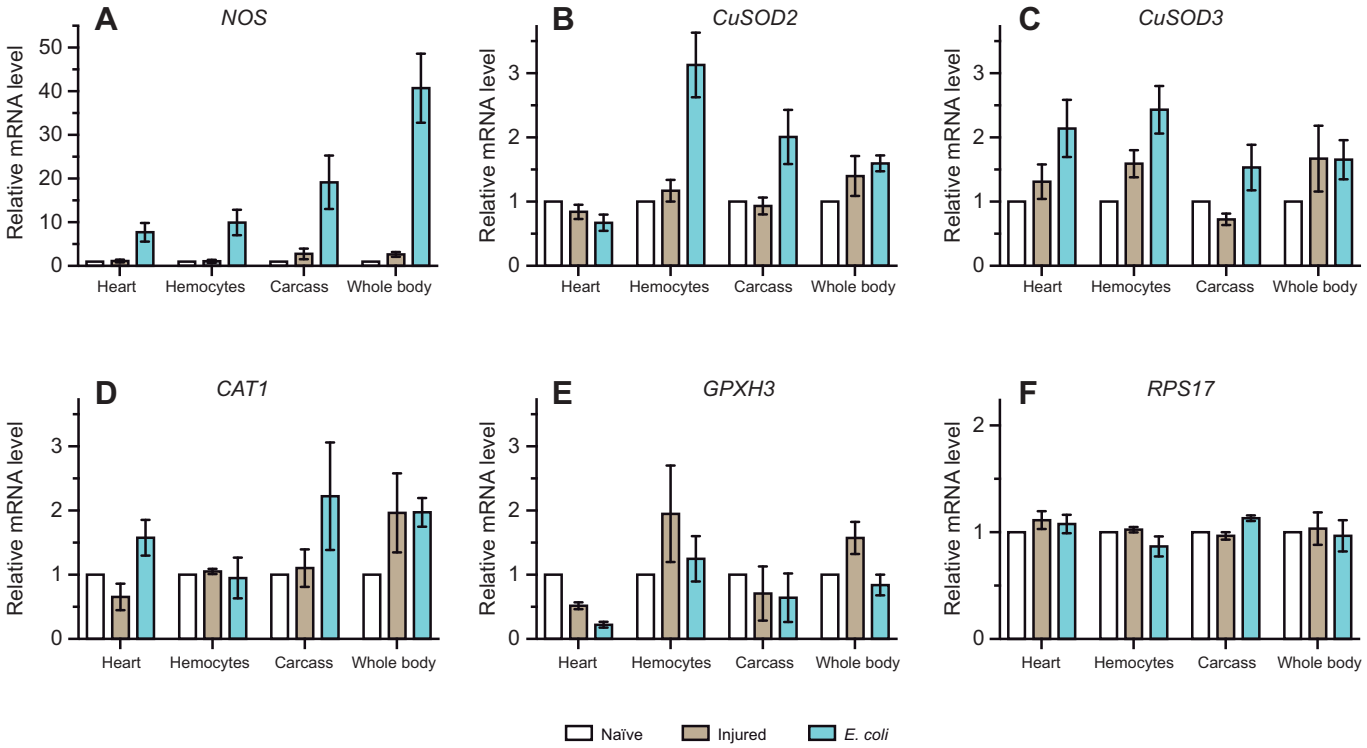

Fig. 5. Effect of infection on the expression of genes encoding enzymes involved in oxidative stress in the heart, hemocytes, carcass and whole body. Relative gene expression of *NOS* (A), *CuSOD2* (B), *CuSOD3* (C), *CAT1* (D), *GPXH3* (E) and *RPS17* (F; control), measured by RT-PCR at 1 day after treatment in naïve, injured and *E. coli*-infected mosquitoes. The graphs display mean±s.e.m. fold-change in mRNA levels relative to the naïve group of each tissue, using *RPS7* as the reference gene. Sample sizes are presented in Table S2.

the percentage of contractions – and the percentage of time spent contracting – in the retrograde direction. Moreover, we discovered that the infection-induced decrease in heart rate is modulated by nitric oxide that is produced by heart-associated periostial hemocytes (Fig. 9).

Prior to the initiation of this work, the effect of infection on heart physiology had only been explored in one study, which found that infection with *E. coli* decreases the heart rate of fruit flies (Broderick et al., 2006). That study, however, is marred by the fact that the flies were anesthetized using FlyNap, which is a volatile mixture that, by itself, modulates heart physiology while at the same time eliminating the cardioacceleratory effect of the neuropeptide, CCAP (Chen and Hillyer, 2013). The present study went further in that it used an anesthetic and immobilization method that does not impact heart physiology (Chen and Hillyer, 2013), and found that infection with any of three different bacterial species decreases the heart rate and increases the percentage of contractions – and the percentage of time spent contracting – in the retrograde direction. We have previously noted that as mosquitoes age there is a similar shift in the proportional directionality of heart contractions, but an infection decreases the heart rate whereas aging increases it (Doran et al., 2017).

We initially hypothesized that the reduced heart rate was because of decreased production of myotropic neuropeptides. Therefore, we queried the transcription of genes that produce them. CCAP is cardioacceleratory in a wide array of insects, including mosquitoes, beetles, moths, fruit flies and stick insects (da Silva et al., 2011; Dulcis et al., 2005; Estevez-Lao et al., 2013; Lehman et al., 1993; Wasielewski and Skonieczna, 2008). FMRFamide-containing peptides are cardioacceleratory in mosquitoes, but in other insects the variable N-terminal sequence determines whether they accelerate or decelerate the heart (Duve et al., 1993; Hillyer et al., 2014; Lee et al., 2012; Nichols, 2006). Corazonin influences cardiac physiology in some insects but not others, and neuropeptide F and short neuropeptide F either affect the heart rate during specific phases of the contraction cycle or have no effect at all (Boerjan et al., 2010; Hillyer et al., 2012; Schiemann et al., 2019; Setzu et al., 2012). In our experiments, the transcription of genes encoding myotropic neuropeptides did not change in a manner that explains the infection-induced cardiac phenotype.

We then turned our attention to nitric oxide because it is a pleiotropic free radical that functions in both defense and circulatory physiology. In vertebrate animals, nitric oxide is a vasodilator and heartbeat reducer (Rastaldo et al., 2007; Smiljic et al., 2014), and is a key contributor to both innate and adaptive immunity (Bogdan, 2015; Rivero, 2006). In stick insects and fruit flies, nitric oxide decreases the heart rate yet in locusts it increases it (Broderick et al., 2006; Bullerjahn et al., 2006; da Silva et al., 2012). Moreover, nitric oxide is an important immune effector in a broad range of insects (Hillyer, 2016). We detected potent transcriptional upregulation of the enzyme that produces nitric oxide (*NOS*) following an infection, and this upregulation was an order of magnitude greater than the transcriptional upregulation of other enzymes involved in oxidative stress. Interestingly, the finding that a decrease in the heart rate is accompanied by an increase in *NOS* mRNA perfectly mirrors what occurs when mosquitoes are starved and dehydrated; depriving mosquitoes of both sucrose and water decreases the heart rate and increases *NOS* transcription without meaningfully affecting the transcription of myotropic neuropeptides (Ellison et al., 2015). Therefore, both the infection and dehydration cardiac phenotypes could be explained by the same, nitric oxide-mediated mechanism. Moreover, the reduction of the heart rate following treatment with

Journal of Experimental Biology (2020) 223, jeb225821. doi:10.1242/jeb.225821

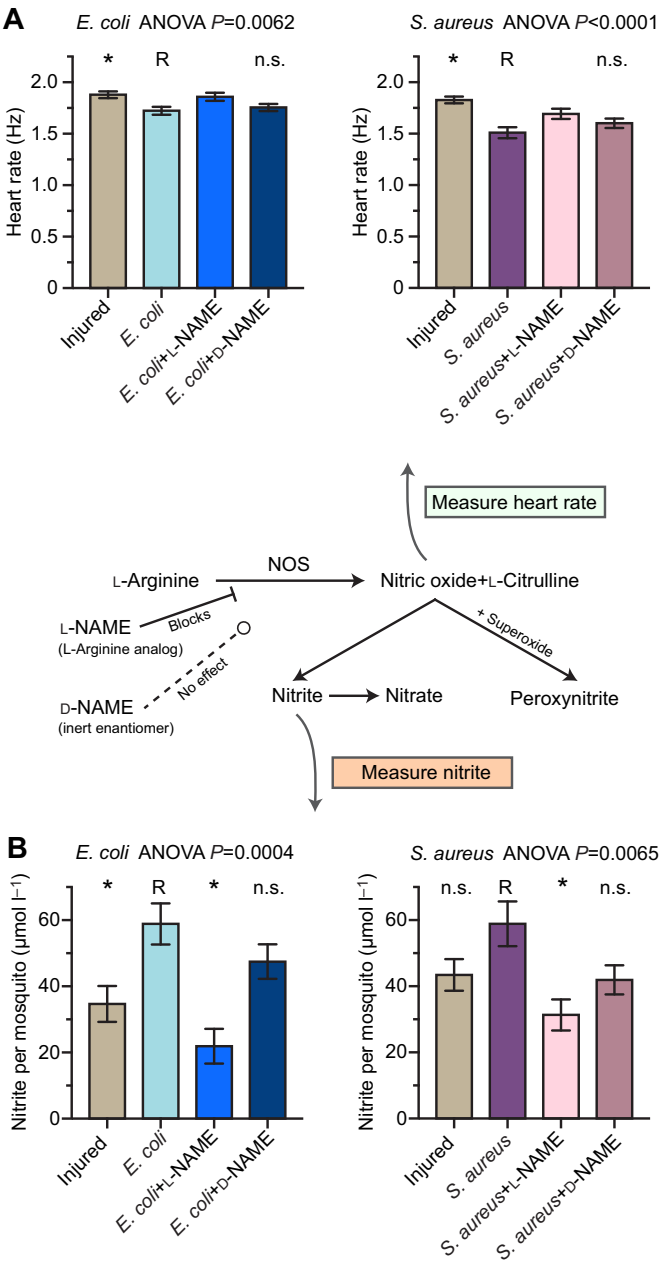

Fig. 6. Effect of inhibiting nitric oxide production on the heart rate and nitrite level in the hemolymph. (A) Heart rate of mosquitoes that were injured, infected with *E. coli* or *S. aureus* for 1 day, or infected with *E. coli* or *S. aureus* for 1 day in the presence of the inhibitor of nitric oxide production, L-NAME, or its inert enantiomer, D-NAME. (B) Level of nitrite in the hemolymph of the mosquitoes outlined for A. The graphs display means±s.e.m. Data were analyzed by one-way ANOVA followed by Dunnett's *post hoc* test. 'R' above a column denotes the reference; **P*<0.05 when compared with the reference; n.s., not significant. Sample sizes are presented in Table S2.

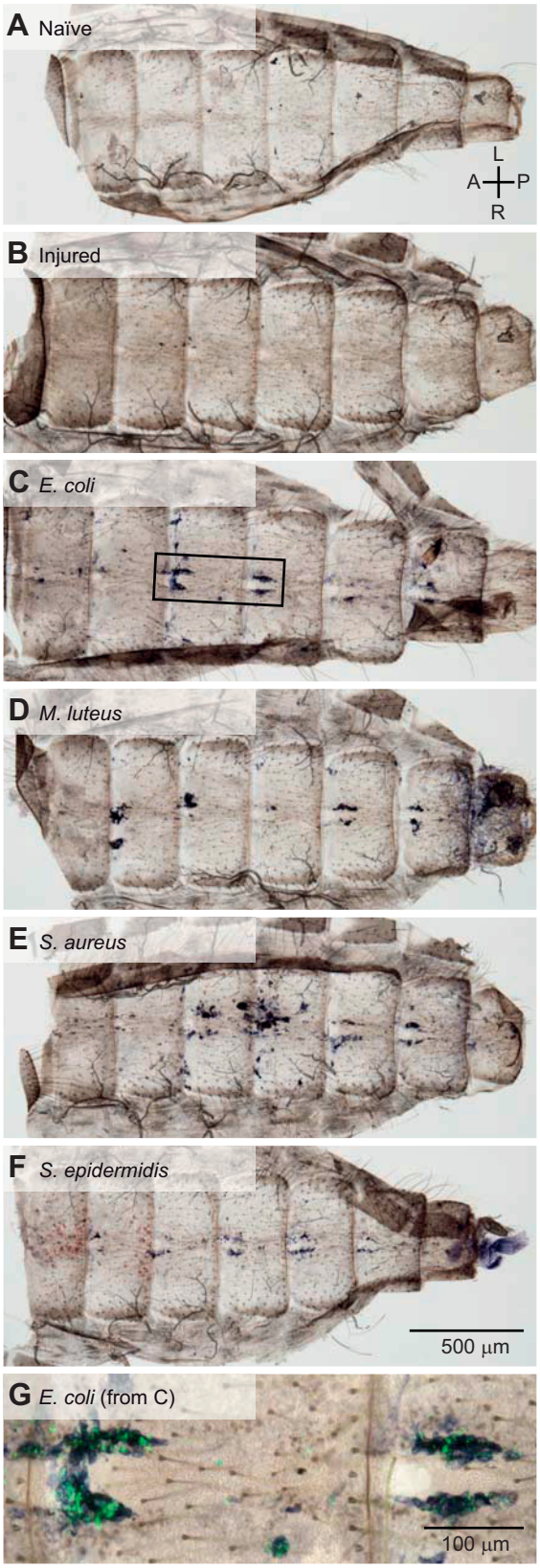

Fig. 7. See next page for legend.

the NOS inhibitor L-NAME mirrors the effect that this chemical has in reducing anti-microbial and anti-malarial activity in the mosquito hemocoel and midgut (Gupta et al., 2009; Hillyer and Estévez-Lao, 2010; Luckhart et al., 1998; Vijay et al., 2011). As for comparing our data across insect species, given the cardiodeceleratory function of nitric oxide in vertebrate animals, we postulate that what occurs in mosquitoes, fruit flies and stick insects – and not what occurs in locusts – represents the ancestral state.

NOS activity in the tergum can only be detected after infection, and only around the heart. This NOS activity is only in periostial hemocytes, and is strongest in the middle abdominal segments. By virtue of being around the ostia, periostial hemocytes are in an

Journal of Experimental Biology (2020) 223, jeb225821. doi:10.1242/jeb.225821

Fig. 7. Effect of infection on nitric oxide synthase activity on the dorsal abdomen. Bright-field microscopy of dorsal abdomens subjected to NADPH diaphorase staining, which marks NOS activity via a blue or purple precipitate. Bright-field images are shown for a naïve mosquito (A), an injured mosquito (B), and mosquitoes infected with *E. coli* (C), *M. luteus* (D), *S. aureus* (E) or *S. epidermidis* (F). In all images, the heart extends from left to right along the midline of the abdomen. (G) Higher magnification image of the highlighted section in panel C; it shows the periostial regions of two abdominal segments. The cells labeled in the periostial regions by diaphorase staining are periostial hemocytes, and the GFP fluorescence channel highlights the recent phagocytosis of *E. coli*. A, anterior; P, posterior; L, left; R, right. The scale bar in F also applies to A–E.

ideal position to sequester and destroy pathogens (King and Hillyer, 2012), and therefore this is an ideal location for nitric oxide to exert its immune – and cardiomodulatory – activity. This interpretation is further supported by the fact that most periostial hemocytes are in the middle abdominal segments, which are the segments that receive the most hemolymph flow (Sigle and Hillyer, 2016). It is also important to note that the circulating hemocytes of mosquitoes, other insects and crustaceans – and the hemocytes contained within the cardiac lumen of stick insects – have NOS activity (da Silva et al., 2012; Hillyer and Estévez-Lao, 2010; Huang et al., 2016; Rodriguez-Ramos et al., 2016), and therefore circulating hemocytes could also contribute to cardiac regulation. When we consider the NOS activity (diaphorase staining) data in light of the *NOS* transcriptional data, we conclude that the increase in *NOS* mRNA in the heart following infection is due to its production by periostial hemocytes and not by cardiac muscle, pericardial cells or any other tissue that associates with the heart.

Having established nitric oxide's involvement in driving the infection-induced cardiac phenotype, we tested whether lysozymes

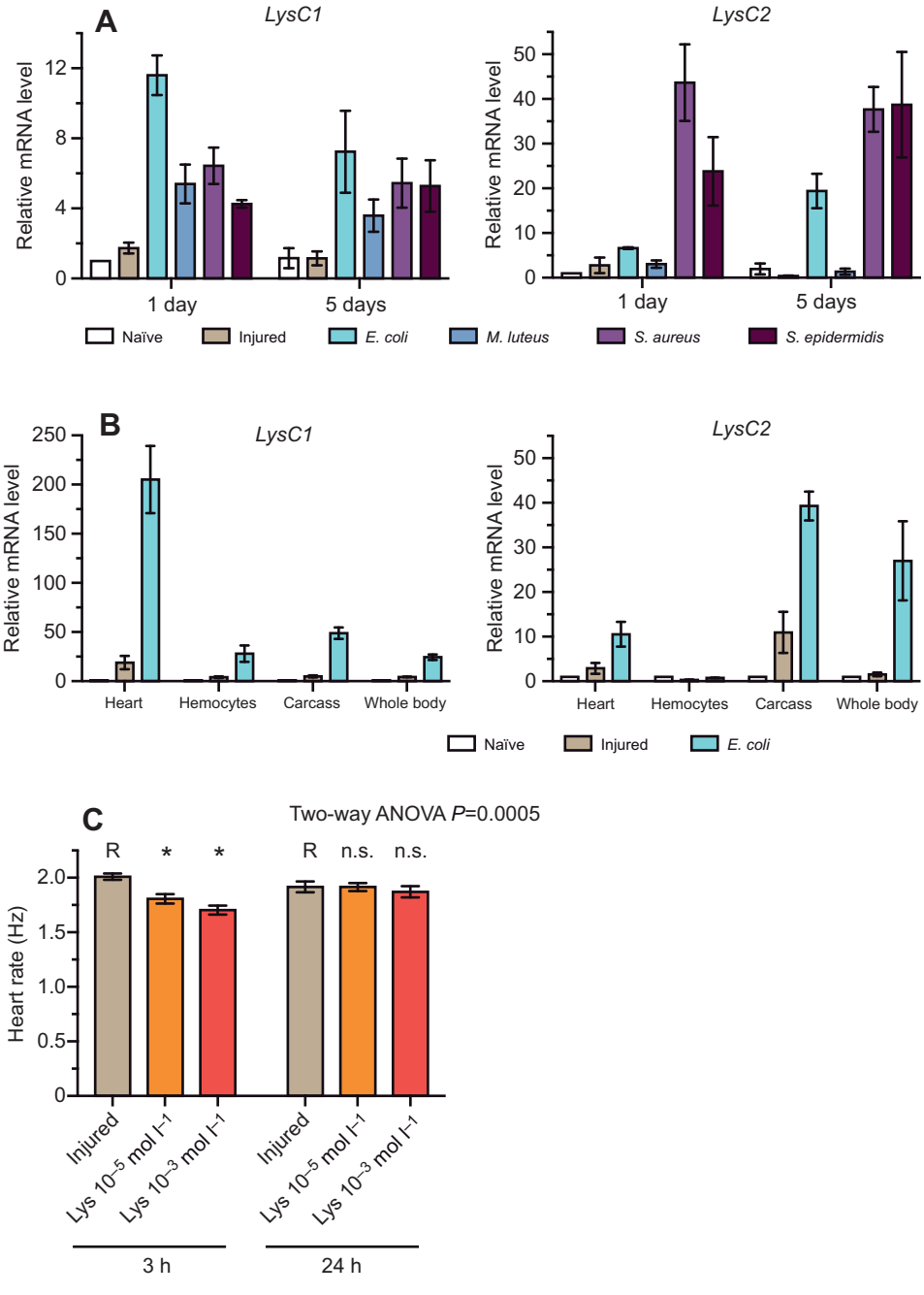

Fig. 8. Effect of infection on lysozyme gene expression and effect of lysozyme on the heart rate. (A,B) *LysC1* and *LysC2* gene expression in the whole body at 1 and 5 days post-treatment (A), and in the heart, hemocytes, carcass and whole body at 1 day post-treatment (B). The graphs display mean±s.e.m. fold-change in mRNA levels relative to naïve mosquitoes at 1 day post-treatment (A) or the naïve group of each tissue (B), using *RPS7* as the reference gene. (C) Heart rate of mosquitoes treated with lysozyme (Lys) for 3 or 24 h. The graphs display means±s.e.m. Data were analyzed by two-way ANOVA followed by Dunnett's *post hoc* test. 'R' above a column denotes the reference; **P*<0.05 when compared with the reference; n.s., not significant. Sample sizes are presented in Table S2.

Journal of Experimental Biology (2020) 223, jeb225821. doi:10.1242/jeb.225821

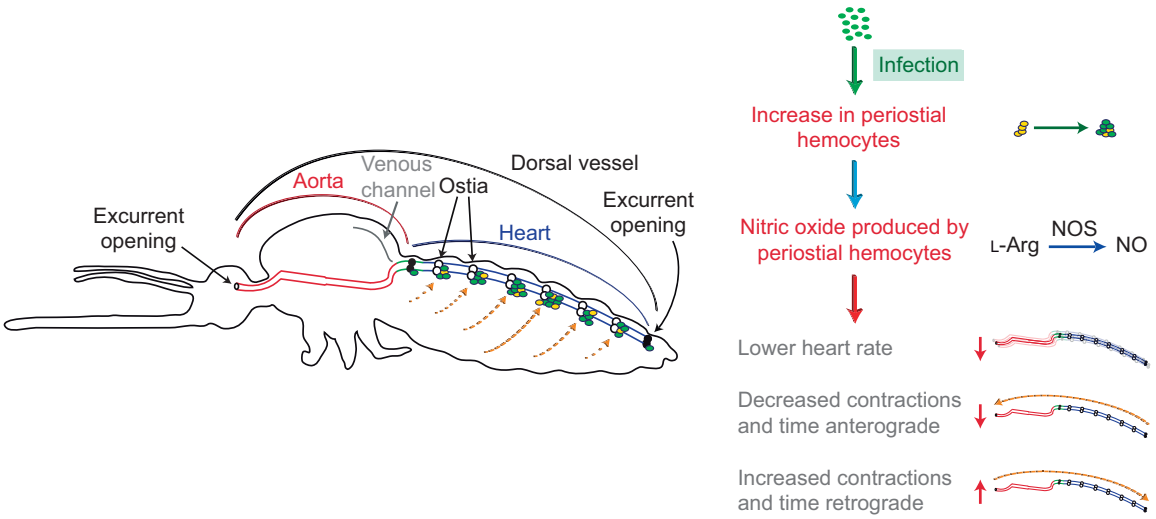

Fig. 9. Diagrammatic representation of a mosquito and the infection-induced modulation of heart physiology.

are also involved. We focused on lysozymes because in canines, cardiovascular dysfunction is affected by lysozymes through a hydrogen peroxide-dependent pathway that appears to activate NOS (Mink et al., 2003, 2009). The *A. gambiae* genome encodes eight lysozyme genes (Li et al., 2005), and our RT-PCR experiments focused on two (*LysC1* and *LysC2*) because they are upregulated after a bacterial infection, and their products are important in the mosquito anti-microbial response (Bartholomay et al., 2007; Brown et al., 2019; Coggins et al., 2012; Kajla et al., 2010; League et al., 2017). We found that *LysC1* is transcriptionally upregulated in hemocytes, which is consistent with the immunocytochemical detection of LysC1 in these cells (Castillo et al., 2006). Moreover, we also uncovered that *LysC1* and *LysC2* are massively upregulated in the heart after infection. Lysozyme mRNA has been detected in the heart of another anopheline species (Hernández-Martínez et al., 2013). However, higher resolution histochemical studies on moths and flies uncovered that pericardial cells, and not the cardiac muscle, contain lysozyme (Crossley, 1972; Russell and Dunn, 1990). When considered together with our transcriptional data, we predict that lysozymes are produced by pericardical cells and additional cells that had not been discovered when the histochemical experiments were conducted: periostial hemocytes. Moreover, when we introduced exogenous lysozyme into mosquitoes, this decreased the heart rate. This appears to be specific to lysozyme and not just the introduction of a protein because injecting sterile growth medium – which is filled with proteins – does not significantly alter the heart rate. The *Drosophila melanogaster* lysozyme, *LySX*, is upregulated in the heart as fruit flies age, and disruption of *LysX* causes bradycardia in an aging heart (Cannon et al., 2017). Therefore, we conclude that lysozymes are immune effectors that regulate cardiac function.

Finally, we detected a slight infection-induced upregulation of enzymes involved in oxidative stress. This upregulation was small compared with nitric oxide or lysozymes, but we do not discount the possibility that these enzymes affect circulatory physiology. Some of the enzymes we assayed have immune function in mosquitoes (Bahia et al., 2013; Herrera-Ortiz et al., 2011; Molina-Cruz et al., 2008; Surachetpong et al., 2011). Moreover, reactive oxygen species drive age-associated changes in the vascular wall of vertebrates, and in fruit flies ROS produced by pericardial cells regulate normal cardiac function (El Assar et al., 2013; Lim et al., 2014).

In conclusion, we discovered that a bacterial infection reduces the heart rate of mosquitoes and biases the proportional directionality of heart contractions. This change in cardiac function is driven by nitric oxide produced by periostial hemocytes that surround the heart's ostia. Taken together, these data demonstrate an exciting new facet of the integration between the immune and circulatory systems of insects.

Acknowledgements
Useful discussions with Yan Yan and Cole Meier are greatly appreciated.

Competing interests
The authors declare no competing or financial interests.

Author contributions
Conceptualization: T.Y.E.-L., J.F.H.; Methodology: T.Y.E.-L., L.T.S., J.F.H.; Validation: T.Y.E.-L., J.F.H.; Formal analysis: T.Y.E.-L., L.T.S., J.F.H.; Investigation: T.Y.E.-L., L.T.S., S.N.G.; Resources: J.F.H.; Data curation: T.Y.E.-L., J.F.H.; Writing - original draft: J.F.H.; Writing - review & editing: T.Y.E.-L., L.T.S., S.N.G., J.F.H.; Visualization: J.F.H.; Supervision: J.F.H.; Project administration: J.F.H.; Funding acquisition: J.F.H.

Funding
This research was funded by US National Science Foundation grant IOS-1456844 to J.F.H.

Supplementary information
Supplementary information available online at
https://jeb.biologists.org/lookup/doi/10.1242/jeb.225821.supplemental

References
Andereck, J. W., King, J. G. and Hillyer, J. F. (2010). Contraction of the ventral abdomen potentiates extracardiac retrograde hemolymph propulsion in the mosquito hemocoel. *PLoS ONE* **5**, e12943. doi:10.1371/journal.pone.0012943

Babcock, D. T., Brock, A. R., Fish, G. S., Wang, Y., Perrin, L., Krasnow, M. A. and Galko, M. J. (2008). Circulating blood cells function as a surveillance system for damaged tissue in *Drosophila* larvae. *Proc. Natl. Acad. Sci. USA* **105**, 10017-10022. doi:10.1073/pnas.0709951105

Bahia, A. C., Oliveira, J. H. M., Kubota, M. S., Araújo, H. R. C., Lima, J. B. P., Ríos-Velásquez, C. M., Lacerda, M. V. G., Oliveira, P. L., Traub-Csekö, Y. M. et al. (2013). The role of reactive oxygen species in *Anopheles aquasalis* response to *Plasmodium vivax* infection. *PLoS ONE* **8**, e57014. doi:10.1371/journal.pone.0057014

Barbosa da Silva, H., Godoy, R. S. M. and Martins, G. F. (2019). The basic plan of the adult heart is conserved across different species of adult mosquitoes, but the morphology of heart-associated tissues varies. *J. Med. Entomol.* **56**, 984-996. doi:10.1093/jme/tjz045

Bartholomay, L. C., Mayhew, G. F., Fuchs, J. F., Rocheleau, T. A., Erickson, S. M., Aliota, M. T. and Christensen, B. M. (2007). Profiling infection responses in the haemocytes of the mosquito, *Aedes aegypti*. *Insect Mol. Biol.* **16**, 761-776. doi:10.1111/j.1365-2583.2007.00773.x

Boerjan, B., Verleyen, P., Huybrechts, J., Schoofs, L. and De Loof, A. (2010). In search for a common denominator for the diverse functions of arthropod corazonin: a role in the physiology of stress? *Gen. Comp. Endocrinol.* **166**, 222-233. doi:10.1016/j.ygcen.2009.09.004

Bogdan, C. (2015). Nitric oxide synthase in innate and adaptive immunity: an update. *Trends Immunol.* **36**, 161-178. doi:10.1016/j.it.2015.01.003

Broderick, K. E., Feala, J., McCulloch, A., Paternostro, G., Sharma, V. S., Pilz, R. B. and Boss, G. R. (2006). The nitric oxide scavenger cobinamide profoundly improves survival in a *Drosophila melanogaster* model of bacterial sepsis. *FASEB J.* **20**, 1865-1873. doi:10.1096/fj.06-5780com

Brown, L. D., Shapiro, L. L. M., Thompson, G. A., Estévez-Lao, T. Y. and Hillyer, J. F. (2019). Transstadial immune activation in a mosquito: adults that emerge from infected larvae have stronger antibacterial activity in their hemocoel yet increased susceptibility to malaria infection. *Ecol. Evol.* **9**, 6082-6095. doi:10.1002/ece3.5192

Brown, L. D., Thompson, G. A. and Hillyer, J. F. (2018). Transstadial transmission of larval hemocoelic infection negatively affects development and adult female longevity in the mosquito *Anopheles gambiae*. *J. Invertebr. Pathol.* **151**, 21-31. doi:10.1016/j.jip.2017.10.008

Bullerjahn, A., Mentel, T., Pflüger, H.-J. and Stevenson, P. A. (2006). Nitric oxide: a co-modulator of efferent peptidergic neurosecretory cells including a unique octopaminergic neurone innervating locust heart. *Cell Tissue Res.* **325**, 345-360. doi:10.1007/s00441-006-0188-2

Cannon, L., Zambon, A. C., Cammarato, A., Zhang, Z., Vogler, G., Munoz, M., Taylor, E., Cartry, J., Bernstein, S. I., Melov, S. et al. (2017). Expression patterns of cardiac aging in *Drosophila*. *Aging Cell* **16**, 82-92. doi:10.1111/acel.12559

Castillo, J. C., Robertson, A. E. Strand, M. R. (2006). Characterization of hemocytes from the mosquitoes *Anopheles gambiae* and *Aedes aegypti*. *Insect Biochem. Mol. Biol.* **36**, 891-903. doi:10.1016/j.ibmb.2006.08.010

Cevik, D., Acker, M., Michalski, C. and Jacobs, J. R. (2019). Pericardin, a *Drosophila* collagen, facilitates accumulation of hemocytes at the heart. *Dev. Biol.* **454**, 52-65. doi:10.1016/j.ydbio.2019.06.006

Chen, W. and Hillyer, J. F. (2013). FlyNap (triethylamine) increases the heart rate of mosquitoes and eliminates the cardioacceleratory effect of the neuropeptide CCAP. *PLoS ONE* **8**, e70414. doi:10.1371/journal.pone.0070414

Chowański, S., Lubawy, J., Urbański, A. and Rosiński, G. (2016). Cardioregulatory functions of neuropeptides and peptide hormones in insects. *Protein Pept. Lett.* **23**, 913-931. doi:10.2174/0929866523666160728102842

Coggins, S. A., Estévez-Lao, T. Y. and Hillyer, J. F. (2012). Increased survivorship following bacterial infection by the mosquito *Aedes aegypti* as compared to *Anopheles gambiae* correlates with increased transcriptional induction of antimicrobial peptides. *Dev. Comp. Immunol.* **37**, 390-401. doi:10.1016/j.dci.2012.01.005

Crossley, A. C. (1972). The ultrastructure and function of pericardial cells and other nephrocytes in an insect: *Calliphora erythrocephala*. *Tissue Cell* **4**, 529-560. doi:10.1016/S0040-8166(72)80029-6

da Silva, S. R., da Silva, R. and Lange, A. B. (2011). Effects of crustacean cardioactive peptide on the hearts of two Orthopteran insects, and the demonstration of a Frank-Starling-like effect. *Gen. Comp. Endocrinol.* **171**, 218-224. doi:10.1016/j.ygcen.2011.01.015

da Silva, R., da Silva, S. R. and Lange, A. B. (2012). The regulation of cardiac activity by nitric oxide (NO) in the Vietnamese stick insect, *Baculum extradentatum*. *Cell. Signal.* **24**, 1344-1350. doi:10.1016/j.cellsig.2012.01.010

Doran, C. R., Estévez-Lao, T. Y. and Hillyer, J. F. (2017). Mosquito aging modulates the heart rate and the proportional directionality of heart contractions. *J. Insect Physiol.* **101**, 47-56. doi:10.1016/j.jinsphys.2017.06.013

Dulcis, D., Levine, R. B. and Ewer, J. (2005). Role of the neuropeptide CCAP in *Drosophila* cardiac function. *J. Neurobiol.* **64**, 259-274. doi:10.1002/neu.20136

Duve, H., Elia, A. J., Orchard, I., Johnsen, A. H. and Thorpe, A. (1993). The effects of CalliFMRFamides and other FMRFamide-related neuropeptides on the activity of the heart of the blowfly *Calliphora vomitoria*. *J. Insect Physiol.* **39**, 31-40. doi:10.1016/0022-1910(93)90015-J

El Assar, M., Angulo, J. and Rodríguez-Mañas, L. (2013). Oxidative stress and vascular inflammation in aging. *Free Radic. Biol. Med.* **65**, 380-401. doi:10.1016/j.freeradbiomed.2013.07.003

Ellison, H. E., Estévez-Lao, T. Y., Murphree, C. S. and Hillyer, J. F. (2015). Deprivation of both sucrose and water reduces the mosquito heart contraction rate while increasing the expression of nitric oxide synthase. *J. Insect Physiol.* **74**, 1-9. doi:10.1016/j.jinsphys.2015.01.011

Estevez-Lao, T. Y., Boyce, D. S., Honegger, H.-W. and Hillyer, J. F. (2013). Cardioacceleratory function of the neurohormone CCAP in the mosquito *Anopheles gambiae*. *J. Exp. Biol.* **216**, 601-613. doi:10.1242/jeb.077164

Ghosh, S., Singh, A., Mandal, S. and Mandal, L. (2015). Active hematopoietic hubs in *Drosophila* adults generate hemocytes and contribute to immune response. *Dev. Cell* **33**, 478-488. doi:10.1016/j.devcel.2015.03.014

Giustarini, D., Rossi, R., Milzani, A. and Dalle-Donne, I. (2008). Nitrite and nitrate measurement by Griess reagent in human plasma: evaluation of interferences and standardization. *Methods Enzymol.* **440**, 361-380. doi:10.1016/S0076-6879(07)00823-3

Glenn, J. D., King, J. G. and Hillyer, J. F. (2010). Structural mechanics of the mosquito heart and its function in bidirectional hemolymph transport. *J. Exp. Biol.* **213**, 541-550. doi:10.1242/jeb.035014

Gonzalez-Zulueta, M., Dawson, V. L. and Dawson, T. M. (1999). Histochemical analysis of nitric oxide synthase by NADPH diaphorase staining. *Curr. Protoc. Toxicol.* **1**, 10.6.1-10.6.4. doi:10.1002/0471140856.tx1006s01

Gorman, M. J. and Paskewitz, S. M. (2000). Persistence of infection in mosquitoes injected with bacteria. *J. Invertebr. Pathol.* **75**, 296-297. doi:10.1006/jipa.2000.4930

Gupta, L., Molina-Cruz, A., Kumar, S., Rodrigues, J., Dixit, R., Zamora, R. E. and Barillas-Mury, C. (2009). The STAT pathway mediates late-phase immunity against *Plasmodium* in the mosquito *Anopheles gambiae*. *Cell Host Microbe* **5**, 498-507. doi:10.1016/j.chom.2009.04.003

Hernández-Martínez, S., Lanz-Mendoza, H., Martinez-Barnetche, J. and Rodríguez, M. H. (2013). Antimicrobial properties of *Anopheles albimanus* pericardial cells. *Cell Tissue Res.* **351**, 127-137. doi:10.1007/s00441-012-1505-6

Herrera-Ortiz, A., Martínez-Barnetche, J., Smit, N., Rodriguez, M. H. and Lanz-Mendoza, H. (2011). The effect of nitric oxide and hydrogen peroxide in the activation of the systemic immune response of *Anopheles albimanus* infected with *Plasmodium berghei*. *Dev. Comp. Immunol.* **35**, 44-50. doi:10.1016/j.dci.2010.08.004

Hillyer, J. F. (2015). Integrated immune and cardiovascular function in Pancrustacea: lessons from the insects. *Integr. Comp. Biol.* **55**, 843-855. doi:10.1093/icb/icv021

Hillyer, J. F. (2016). Insect immunology and hematopoiesis. *Dev. Comp. Immunol.* **58**, 102-118. doi:10.1016/j.dci.2015.12.006

Hillyer, J. F. (2018). Insect heart rhythmicity is modulated by evolutionarily conserved neuropeptides and neurotransmitters. *Curr. Opin. Insect Sci.* **29**, 41-48. doi:10.1016/j.cois.2018.06.002

Hillyer, J. F. and Christensen, B. M. (2002). Characterization of hemocytes from the yellow fever mosquito, *Aedes aegypti*. *Histochem. Cell Biol.* **117**, 431-440. doi:10.1007/s00418-002-0408-0

Hillyer, J. F. and Estévez-Lao, T. Y. (2010). Nitric oxide is an essential component of the hemocyte-mediated mosquito immune response against bacteria. *Dev. Comp. Immunol.* **34**, 141-149. doi:10.1016/j.dci.2009.08.014

Hillyer, J. F. and Pass, G. (2020). The insect circulatory system: structure, function, and evolution. *Annu. Rev. Entomol.* **65**, 121-143. doi:10.1146/annurev-ento-011019-025003

Hillyer, J. F., Estévez-Lao, T. Y. and de la Parte, L. E. (2014). Myotropic effects of FMRFamide containing peptides on the heart of the mosquito *Anopheles gambiae*. *Gen. Comp. Endocrinol.* **202**, 15-25. doi:10.1016/j.ygcen.2014.03.048

Hillyer, J. F., Estévez-Lao, T. Y., Funkhouser, L. J. and Aluoch, V. A. (2012). *Anopheles gambiae* corazonin: gene structure, expression and effect on mosquito heart physiology. *Insect Mol. Biol.* **21**, 343-355. doi:10.1111/j.1365-2583.2012.01140.x

Horn, L., Leips, J. and Starz-Gaiano, M. (2014). Phagocytic ability declines with age in adult *Drosophila* hemocytes. *Aging Cell* **13**, 719-728. doi:10.1111/acel.12227

Huang, Q., Zhang, L., Yang, C., Yun, X. and He, Y. (2016). The competence of hemocyte immunity in the armyworm *Mythimna separata* larvae to sublethal hexaflumuron exposure. *Pestic. Biochem. Physiol.* **130**, 31-38. doi:10.1016/j.pestbp.2015.12.003

Hughes, M. N. (2008). Chemistry of nitric oxide and related species. *Methods Enzymol.* **436**, 3-19. doi:10.1016/S0076-6879(08)36001-7

Kajla, M. K., Andreeva, O., Gilbreath, T. M., , III and Paskewitz, S. M. (2010). Characterization of expression, activity and role in antibacterial immunity of *Anopheles gambiae* lysozyme c-1. *Comp. Biochem. Physiol. B Biochem. Mol. Biol.* **155**, 201-209. doi:10.1016/j.cbpb.2009.11.012

Kelm, M. (1999). Nitric oxide metabolism and breakdown. *Biochim. Biophys. Acta* **1411**, 273-289. doi:10.1016/S0005-2728(99)00020-1

King, J. G. and Hillyer, J. F. (2012). Infection-induced interaction between the mosquito circulatory and immune systems. *PLoS Pathog.* **8**, e1003058. doi:10.1371/journal.ppat.1003058

King, J. G. and Hillyer, J. F. (2013). Spatial and temporal *in vivo* analysis of circulating and sessile immune cells in mosquitoes: hemocyte mitosis following infection. *BMC Biol.* **11**, 55. doi:10.1186/1741-7007-11-55

Lai, S.-C., Chen, C.-C. and Hou, R. F. (2001). Electron microscopic observations on wound-healing in larvae of the mosquito *Armigeres subalbatus* (Diptera: Culicidae). *J. Med. Entomol.* **38**, 836-843. doi:10.1603/0022-2585-38.6.836

League, G. P. and Hillyer, J. F. (2016). Functional integration of the circulatory, immune, and respiratory systems in mosquito larvae: pathogen killing in the hemocyte-rich tracheal tufts. *BMC Biol.* **14**, 78. doi:10.1186/s12915-016-0305-y

League, G. P., Estévez-Lao, T. Y., Yan, Y., Garcia-Lopez, V. A. and Hillyer, J. F. (2017). *Anopheles gambiae* larvae mount stronger immune responses against bacterial infection than adults: evidence of adaptive decoupling in mosquitoes. *Parasit. Vectors* **10**, 367. doi:10.1186/s13071-017-2302-6

League, G. P., Onuh, O. C. and Hillyer, J. F. (2015). Comparative structural and functional analysis of the larval and adult dorsal vessel and its role in hemolymph circulation in the mosquito *Anopheles gambiae*. *J. Exp. Biol.* **218**, 370-380. doi:10.1242/jeb.114942

Lee, D., Taufique, H., da Silva, R. and Lange, A. B. (2012). An unusual myosuppressin from the blood-feeding bug *Rhodnius prolixus*. *J. Exp. Biol.* **215**, 2088-2095. doi:10.1242/jeb.067447

Lehman, H. K., Murgiuc, C. M., Miller, T. A., Lee, T. D. and Hildebrand, J. G. (1993). Crustacean cardioactive peptide in the sphinx moth, *Manduca sexta*. *Peptides* **14**, 735-741. doi:10.1016/0196-9781(93)90106-Q

Li, B., Calvo, E., Marinotti, O., James, A. A. and Paskewitz, S. M. (2005). Characterization of the c-type lysozyme gene family in *Anopheles gambiae*. *Gene* **360**, 131-139. doi:10.1016/j.gene.2005.07.001

Lim, H.-Y., Wang, W., Chen, J., Ocorr, K. and Bodmer, R. (2014). ROS regulate cardiac function via a distinct paracrine mechanism. *Cell Rep.* **7**, 35-44. doi:10.1016/j.celrep.2014.02.029

Livak, K. J. and Schmittgen, T. D. (2001). Analysis of relative gene expression data using real-time quantitative PCR and the 2(-ΔΔC(T)) method. *Methods* **25**, 402-408. doi:10.1006/meth.2001.1262

Luckhart, S., Vodovotz, Y., Cui, L. and Rosenberg, R. (1998). The mosquito *Anopheles stephensi* limits malaria parasite development with inducible synthesis of nitric oxide. *Proc. Natl. Acad. Sci. USA* **95**, 5700-5705. doi:10.1073/pnas.95.10.5700

Mink, S. N., Jacobs, H., Bose, D., Duke, K., Cheng, Z. Q., Liu, G. and Light, R. B. (2003). Lysozyme: a mediator of myocardial depression and adrenergic dysfunction in septic shock in dogs. *J. Mol. Cell. Cardiol.* **35**, 265-275. doi:10.1016/S0022-2828(03)00004-X

Mink, S. N., Jacobs, H., Cheng, Z.-Q., Kasian, K., Santos-Martinez, L. E. and Light, R. B. (2009). Lysozyme, a mediator of sepsis that intrinsically generates hydrogen peroxide to cause cardiovascular dysfunction. *Am. J. Physiol. Heart Circ. Physiol.* **297**, H930-H948. doi:10.1152/ajpheart.00732.2008

Molina-Cruz, A., DeJong, R. J., Charles, B., Gupta, L., Kumar, S., Jaramillo-Gutierrez, G. and Barillas-Mury, C. (2008). Reactive oxygen species modulate *Anopheles gambiae* immunity against bacteria and *Plasmodium*. *J. Biol. Chem.* **283**, 3217-3223. doi:10.1074/jbc.M705873200

Nichols, R. (2006). FMRFamide-related peptides and serotonin regulate *Drosophila melanogaster* heart rate: mechanisms and structure requirements. *Peptides* **27**, 1130-1137. doi:10.1016/j.peptides.2005.07.032

Pereira, M. F., Rossi, C. C., de Queiroz, M. V., Martins, G. F., Isaac, C., Bosse, J. T., Li, Y., Wren, B. W., Terra, V. S., Cuccui, J. et al. (2015). *Galleria mellonella* is an effective model to study *Actinobacillus pleuropneumoniae* infection. *Microbiology* **161**, 387-400. doi:10.1099/mic.0.083923-0

Rastaldo, R., Pagliaro, P., Cappello, S., Penna, C., Mancardi, D., Westerhof, N. and Losano, G. (2007). Nitric oxide and cardiac function. *Life Sci.* **81**, 779-793. doi:10.1016/j.lfs.2007.07.019

Rees, D. D., Palmer, R. M. J., Schulz, R., Hodson, H. F. and Moncada, S. (1990). Characterization of three inhibitors of endothelial nitric oxide synthase *in vitro* and *in vivo*. *Br. J. Pharmacol.* **101**, 746-752. doi:10.1111/j.1476-5381.1990.tb14151.x

Richards, A. G. (1963). The effect of temperature on heart-beat frequency in the cockroach, *Periplaneta americana*. *J. Insect Physiol.* **9**, 597-606. doi:10.1016/0022-1910(63)90005-2

Rivero, A. (2006). Nitric oxide: an antiparasitic molecule of invertebrates. *Trends Parasitol.* **22**, 219-225. doi:10.1016/j.pt.2006.02.014

Rodriguez-Ramos, T., Carpio, Y., Bolivar, J., Gomez, L., Estrada, M. P. and Pendon, C. (2016). Nitric oxide synthase-dependent immune response against gram negative bacteria in a crustacean, *Litopenaeus vannamei*. *Fish Shellfish Immunol.* **50**, 50-55. doi:10.1016/j.fsi.2016.01.019

Russell, V. W. and Dunn, P. E. (1990). Lysozyme in the pericardial complex of *Manduca sexta*. *Insect Biochem.* **20**, 501-509. doi:10.1016/0020-1790(90)90032-P

Schiemann, R., Lammers, K., Janz, M., Lohmann, J., Paululat, A. and Meyer, H. (2019). Identification and *in vivo* characterisation of cardioactive peptides in *Drosophila melanogaster*. *Int. J. Mol. Sci.* **20**, 2. doi:10.3390/ijms20010002

Setzu, M., Biolchini, M., Lilliu, A., Manca, M., Muroni, P., Poddighe, S., Bass, C., Angioy, A. M. and Nichols, R. (2012). Neuropeptide F peptides act through unique signaling pathways to affect cardiac activity. *Peptides* **33**, 230-239. doi:10.1016/j.peptides.2012.01.005

Sigle, L. T. and Hillyer, J. F. (2016). Mosquito hemocytes preferentially aggregate and phagocytose pathogens in the periostial regions of the heart that experience the most hemolymph flow. *Dev. Comp. Immunol.* **55**, 90-101. doi:10.1016/j.dci.2015.10.018

Sigle, L. T. and Hillyer, J. F. (2018a). Mosquito hemocytes associate with circulatory structures that support intracardiac retrograde hemolymph flow. *Front. Physiol.* **9**, 1187. doi:10.3389/fphys.2018.01187

Sigle, L. T. and Hillyer, J. F. (2018b). Structural and functional characterization of the contractile aorta and associated hemocytes of the mosquito *Anopheles gambiae*. *J. Exp. Biol.* **221**, jeb181107. doi:10.1242/jeb.181107

Smiljic, S., Nestorovic, V. and Savic, S. (2014). Modulatory role of nitric oxide in cardiac performance. *Med. Pregl.* **67**, 345-352. doi:10.2298/MPNS1410345S

Surachetpong, W., Pakpour, N., Cheung, K. W. and Luckhart, S. (2011). Reactive oxygen species-dependent cell signaling regulates the mosquito immune response to *Plasmodium falciparum*. *Antioxid. Redox Signal.* **14**, 943-955. doi:10.1089/ars.2010.3401

Vijay, S., Rawat, M., Adak, T., Dixit, R., Nanda, N., Srivastava, H., Sharma, J. K., Prasad, G. B. K. S. and Sharma, A. (2011). Parasite killing in malaria non-vector mosquito *Anopheles culicifacies* species B: implication of nitric oxide synthase upregulation. *PLoS ONE* **6**, e18400. doi:10.1371/journal.pone.0018400

Wasielewski, O. and Skonieczna, M. (2008). Pleiotropic effects of the neuropeptides CCAP and myosuppressin in the beetle, *Tenebrio molitor* L. *J. Comp. Physiol. B* **178**, 877-885. doi:10.1007/s00360-008-0276-6

Table S1. Information on primers used for RT-PCR.

Gene	VectorBase ID[a]	Sequence (forward [top] and reverse [bottom])	Amplicon (bp)[b,c]	
			Transcript	Genomic
RPS7	AGAP010592	GACGGATCCCAGCTGATAAA	132	281
		GTTCTCTGGGAATTCGAACG		
RPS17	AGAP004887	GACGAAACCACTGCGTAACA	153	264
		TGCTCCAGTGCTGAAACATC		
NOS	AGAP029502	CAAGAGTGGGACCACATCAA	129	210
		ACCCTTCTGGACCATCTCCT		
LYSC1	AGAP007347	ACGGCATCTTCCAGATCAAC	180	259
		CATTGCAGTGGTTCTTCCAG		
LYSC2	AGAP007343	AAGAAATTGTTGCCGGATTG	172	247
		TTTGGCACGGTATATTGCAC		
CAT1	AGAP004904	ACGGAAAACAAATCCCATCA	188	7533
		GTCGATCAGGTGAACGTCCT		
CuSOD2	AGAP005234	ATTGCTCTATCGACCGTGCT	198	1067
		ACCCTTCTCGTGAATGTGGA		
CuSOD3	AGAP010347	CCACAGTTTTGTTCGTGACA	200	200
		CCTTCACTTCTCCGTTCAGC		
GPXH3	AGAP004248	ACGAAATCGTACAGCGCTTC	181	1008
		CGGTCGGTAAGAAAGATGGT		
CCAP	AGAP009729	GCTGGCAGTTGTATCGCTCT	127	201
	JX880074	GGTAAAGGCGTTGCAGAAC		
CRZ	AGAP003675	AGTACTCCCGTGGATGGACA	171	NA
		GTCGTAGGAGCGCTTTTTCA		
FMRFamide	AGAP005518	TTTACATACGGCGTGACTCG	229	229
	KJ583231, KJ583232	CCAAAGCGCATCAGATTACC		
NPF	AGAP004642	TTACTCAGCGTTTGCTGGTG	170	NA
		TCCGAATCTGGGTCTAGCAT		
sNPF	DQ437578	GCTGTTAGTCCTCGCGGTAG	180	UNK
		CTTCCAAACCGTAGCCTCAG		

a IDs are from the AgamP4 assembly in www.vectorbase.org (AGAP) or from www.ncbi.nlm.nih.gov/genbank (JX; KJ; DQ).
b Amplicon sizes are based on the sequences in Vectorbase or Genbank.
c "NA" indicates the primer span an exon-intron junction, thus unable to amplify from genomic DNA. "UNK" means that the size of the genomic amplicon is unknown.

Table S2. Sample sizes for figures 1-6 and 8

Figure 1: Panels A-H

	Naïve	Injured	*E. coli*	*M. luteus*	*S. aureus*	*S. epidermidis*
1 day	77	80	73	59	56	45
3 days	28	30	30	29	30	19
5 days	24	26	27	18	18	16

Figure 2: Panels A and C

	Naïve	Injured	*E. coli*	*M. luteus*	*S. aureus*	*S. epidermidis*
1 day	5	5	5	5	5	5
5 days	4	4	4	4	4	4

Figure 2: Panel B

	Naïve	Injured	*E. coli*	*M. luteus*	*S. aureus*	*S. epidermidis*
1 day	5	5	5	5	5	4
5 days	4	4	4	4	4	4

Figure 2: Panels D and E

	Naïve	Injured	*E. coli*	*M. luteus*	*S. aureus*	*S. epidermidis*
1 day	3	3	3	3	3	3
5 days	3	3	3	3	3	3

Figure 3: Panels A-E

	Naïve	Injured	*E. coli*
Heart	3	3	3
Hemocytes	2	2	2
Carcass	3	3	3
Whole Body	3	3	3

Figure 4: Panels A

	Naïve	Injured	*E. coli*	*M. luteus*	*S. aureus*	*S. epidermidis*
1 day	5	5	5	5	5	5
5 days	4	4	4	4	4	4

Figure 4: Panels B-F

	Naïve	Injured	*E. coli*	*M. luteus*	*S. aureus*	*S. epidermidis*
1 day	3	3	3	3	3	3
5 days	3	3	3	3	3	3

Figure 5: Panels A-F

	Naïve	Injured	*E. coli*
Heart	3	3	3
Hemocytes	2	2	2
Carcass	3	3	3
Whole Body	3	3	3

Table S2 (Continued). Sample sizes for figures 1-6 and 8

Figure 6: Panel A

	E. coli	*S. aureus*
Injured	25	26
Infection	27	26
Infection + L-NAME	27	23
Infection + D-NAME	26	26

Figure 6: Panel B

	E. coli	*S. aureus*
Injured	8	12
Infection	8	12
Infection + L-NAME	8	12
Infection + D-NAME	8	12

Figure 8: Panel A (*LysC1*)

	Naïve	Injured	*E. coli*	*M. luteus*	*S. aureus*	*S. epidermidis*
1 day	3	3	3	3	3	3
5 days	3	3	3	3	3	3

Figure 8: Panel A (*LysC2*)

	Naïve	Injured	*E. coli*	*M. luteus*	*S. aureus*	*S. epidermidis*
1 day	2	2	2	2	2	2
5 days	2	2	2	2	2	2

Figure 8: Panel B (*LysC1* and *LysC2*)

	Naïve	Injured	*E. coli*
Heart	3	3	3
Hemocytes	2	2	2
Carcass	3	3	3
Whole Body	3	3	3

Figure 8: Panel C

	Injured	Lys 10^{-5} M	Lys 10^{-3} M
3 hours	23	26	23
24 hours	26	27	27